Highly Directional Emission from Inhomogeneous Dielectric Microcavities

G. Painchaud-April[1], J. Poirier[1], S. Saïdi[2], Y.-A. Peter[2], E. Brasselet[3], L. J. Dubé[1]

[1]*Département de Physique, de Génie Physique, et d'Optique, Université Laval, Québec, Canada*
[2]*Laboratoire de Micro et Nano Systèmes, Département de Génie Physique, Ecole Polytechnique de Montréal, Montréal, Québec*
[3]*Centre de Physique Moléculaire, Optique et Hertzienne, Université Bordeaux I, France*

We propose a novel method of extracting light beams from 2D microcavities. The concept is based on inhomogeneous dielectric cavities (IDC) where the inhomogeneities arise from a space-dependent refractive index whose variations may be continuous (e.g. a localized induced gaussian profile of the index) or discontinuous (e.g. holes or refractive steps in the cavity material). Instead of the so-called asymmetric resonant cavities (ARC), which are smooth deformations of a circular cavity and produce directional output while sacrificing the quality factor Q, we intend to operate with an integrable geometry (a disk) and induce directionality through the (possibly reconfigurable) medium while preserving a high Q. The systems are interesting on two counts. Firstly, as classical objects, the IDC are equivalent to dielectric billiards (i.e. photonic escape is possible) where the broken symmetry of the material can induce a transition from regular to chaotic dynamics: chaos in an integrable billiard geometry, an almost unique combination. Secondly, guided by the classical phase space information, the wave dynamics can be "engineered" to produce highly directional emission with tailored optical properties, the grail of microcavity research. We have studied a number of configurations and will present results on their respective performances.

System description

For ***optically thin systems****, we obtain Helmholtz equation for the transverse magnetic (TM) polarization (electric field ψ along Oz axis)*

$$\left[\nabla^2 + n^2(\mathbf{r})k^2\right]\psi = 0, \ \mathbf{r} \in \mathbb{R}^2 \qquad (1)$$

where

$$n(\mathbf{r}) = \begin{cases} n_{\text{in}}(\mathbf{r}) & \mathbf{r} \in \Omega_c \\ n_{\text{ex}}(\mathbf{r}) = \text{const} & \mathbf{r} \in \mathbb{R}^2 \backslash \Omega_c \end{cases} \qquad (2)$$

is the (real) refractive index and k, the wavenumber. The region Ω_c with boundary $\partial\Omega_c$ defines the ***cavity****. The field on $\partial\Omega_c$ must satisfy continuity up to the first normal derivative:*

- *Continuity:* $\psi|_{\partial\Omega_c^+} = \psi|_{\partial\Omega_c^-}$,
- *Normal derivative continuity:* $\partial_n\psi|_{\partial\Omega_c^+} = \partial_n\psi|_{\partial\Omega_c^-}$.

In the exterior region, equation (1) may be solved exactly in polar coordinates in terms of ***partial waves***

$$\psi(\mathbf{r}) = \sum_l \left[A_l H_l^{(2)}(n_{\text{ex}}kr) + B_l H_l^{(1)}(n_{\text{ex}}kr)\right] e^{il\phi} \qquad (3)$$

*where $H_\nu^{(1,2)}(z)$ are Hankel functions of first and second kind. These functions are especially well suited to meet outgoing and incoming wave conditions for large arguments (****Far Field region*** *(FF), $r \to \infty$):*

$$H_\nu^{(j)}(z) \sim \sqrt{\frac{2}{\pi z}}\exp[(-1)^j i(-z + \nu\pi/2) - i\pi/4] \quad . \qquad (4)$$

Two conceptually different approaches can be used to extract modal characteristics of the field:

- ***Emission approach****: The field is supposed to have existed inside the cavity since $t \to -\infty$: $\{A_l\} = 0$ (no incoming field), $k \in \mathbb{C}$, $\text{Im}\{k\} < 0$ in (3),*
- ***Scattering approach****: The incoming field is a continuous wave: $\{A_l\} \neq 0$ at least for some l, $k \in \mathbb{R}$.*

Scattering approach

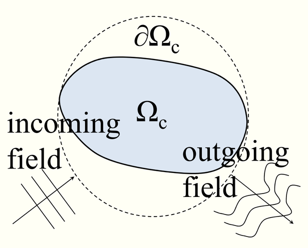

Fig. 1: **Scattering approach for resonant mode calculation.**

The pivotal quantity of the scattering theory is the ***scattering matrix*** **S** *whose elements S_{ij} are probability amplitudes connecting incoming partial wave j to outgoing partial wave i. Once calculated [1], this matrix can be used to express the outgoing wave relative to the incoming one. We choose the incident wave according to the eigenstates of* ***mean electromagnetic energy matrix*** *[2]*

$$\mathbf{Q} = -i\mathbf{S}^\dagger\frac{\partial\mathbf{S}}{\partial k} \quad . \qquad (5)$$

Normalizing the incoming energy flux enables us to compare energy levels of those "energy modes": the ***more energy*** *gets trapped inside the cavity, the* ***longer the residence time*** *(****delay****) of the corresponding mode, and hence, the* ***higher the quality factor****. Of particular interest are* ***resonant states*** *which maximize the stored electromagnetic energy.*

[1] A. I. Rahachou and I. V. Zozoulenko, Appl. Opt, **43** (2004), 1761-1772

[2] F. T. Smith, Phys. Rev, **118** (1960), 349-356

A difficult compromise

Historically, the first optical 2D microresonators were of ***symmetrical shape*** *(microdisks): their corresponding classical billiard phase space is completely* ***integrable****. They are characterized by* ***high quality modes*** *($Q \gg 1$) of* ***isotropic emission*** *in the FF region. In order to obtain directional emission in FF, it has been considered to* ***geometrically deform*** *the cavity: many geometries have been proposed such as quadrupolar and stadium shapes. The end result is a* ***gain in directionality*** *and important* ***losses in quality factor****.*

Recent developments in the understanding of transport properties of quantum (wave) billiards [3] suggest that it is possible to couple two modes of a given cavity and to obtain a ***hybrid state*** *exhibiting characteristics of both. We are then led to reconsider the integrable disk cavity (high quality modes) with enclosed defects leading to disruption of underlying phase space regular structures and* ***emergence of classical chaos****. To illustrate our point, we have chosen, out of simplicity, the* ***annular cavity****.*

[3] J. Wiersig and M. Hentschel, Phys. Rev. Lett, **100** (2008), 033901-4

The annular cavity

The annular cavity consists in a disk cavity (n_{in} = const) with a circular hole ($n_{\text{hole}} = n_{\text{ex}}$) located at a distance d from the geometrical center of Ω_c (see Fig. 2). The Whispering Gallery Modes (WGMs) of the disk cavity

$$\psi_{\text{WGMs}}(\mathbf{r}) \sim J_m(n_{\text{in}}kr)e^{im\phi} \qquad (6)$$

may still be found in the annular cavity if their centermost extremum is located inside the "safe zone" of radial length $\alpha = R_0 - (d + R_1)$ (see Fig. 3 and 4).

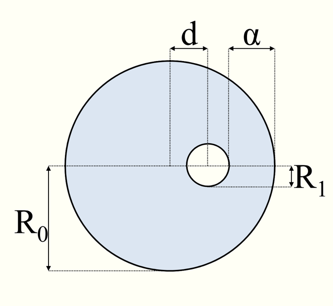

Fig. 2: **Construction of annular cavity. Parameter α is critical for WGMs.**

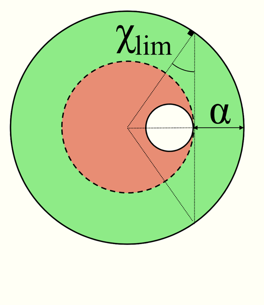

Fig. 3: **Green region can withstand WGMs. Modes inside red region are likely to be chaotic.**

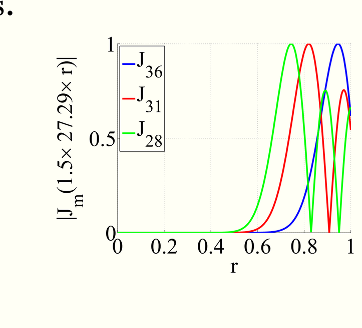

Fig. 4: **Some $J_m(nkr)$ Bessel functions with n = 1.5 and k = 27.29.**

Correspondingly, we find a limit angle at which a classical particle might impact the inner circle (hole)

$$\sin\chi_{\text{lim}} \equiv (R_0 - \alpha)/R_0 \qquad (7)$$

hence defining a

- ***Regular region****:* $|p| > \sin\chi_{\text{lim}}$,
- ***Mixed region****:* $|p| < \sin\chi_{\text{lim}}$

with $p = \sin\chi$ the canonical momentum coordinate. Because of ***dynamical tunnelling****, the WGMs located above the line $\sin\chi_{\text{lim}}$ in classical phase space (ϕ, p) may connect with modes in the chaotic region below. These modes being partially localized inside emission region limited by the lines $|\sin\chi_c| = n_{\text{ex}}/n_{\text{in}}$, the FF is then strongly influenced by them. Such behaviour in depicted by the* ***Husimi distribution*** *restricted to emission region.*

Numerical results

We present results of scattering numerical simulations on annular cavity. We set $n_{\text{in}} = 1.5$, $n_{\text{ex}} = 1$, $R_0 = 1$, $R_1 = 0.3$ and use d (or α) ranging from 0.35 to 0.55 as a ***control parameter****. Fig. 5 present delay values ($\propto$ stored energy) for eigenstates of reference circular cavity in region $k = [26.5, \ 28.5]$. We select WGM $(36, 1)$ as our high Q mode (with regards to equation (6), $m = 36$ and 1 is the number of radial maxima inside Ω_c).*

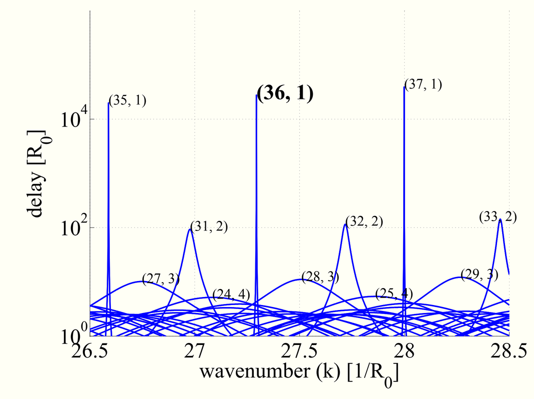

Fig. 5: **Delay spectrum for the disk cavity. Mode $(36, 1)$ is highlighted.**

Husimi distributions and FF patterns for mode $(36, 1)$ are shown in Fig. 6 for 3 increasing values of d. Although delay time suffers a significative loss of a factor ~ 20 from $d = 0.35$ to $d = 0.55$, the mode at $d = 0.50$ is only slightly affected (factor 2) while presenting peaks along well-defined directions.

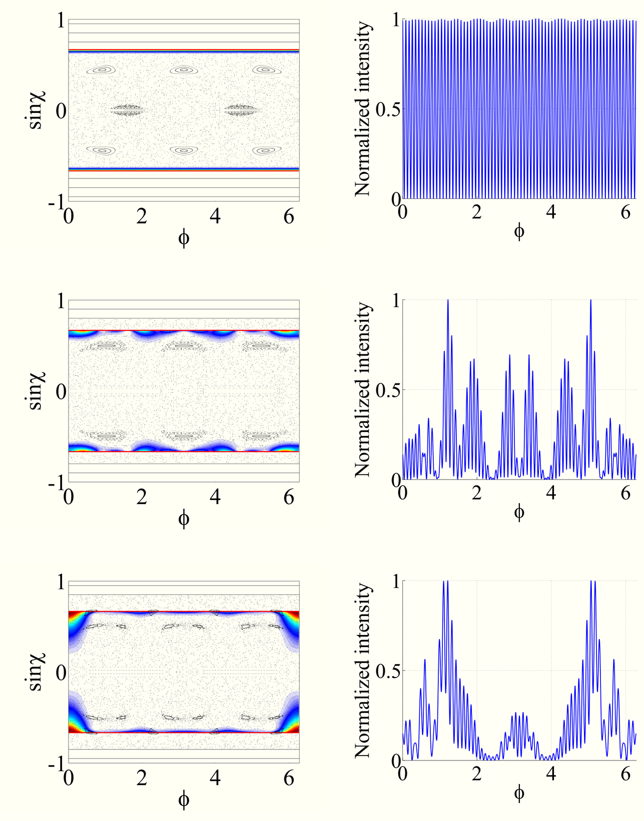

Fig. 6: **(Left) Husimi distribution in emission area of phase space (Red line: Total internal reflection limit) and (Right) FF pattern of corresponding mode. Top to bottom: $d = \{0.35, \ 0.50, \ 0.55\}$.**

Experimental results

Encouraging advances in fabrication of microcavities let foresee technological applications of high Q directional cavities. New medium deformations might be designed to optimize or possibly dynamically control directional emission.

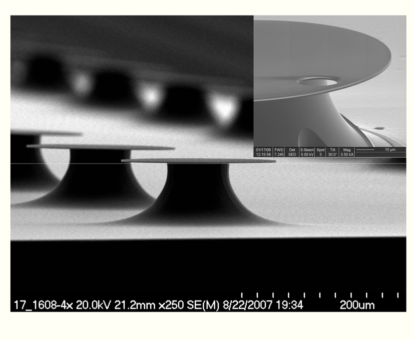

Fig. 7: **Disk cavities. Inset: An annular cavity with hole radius of 5μm.**

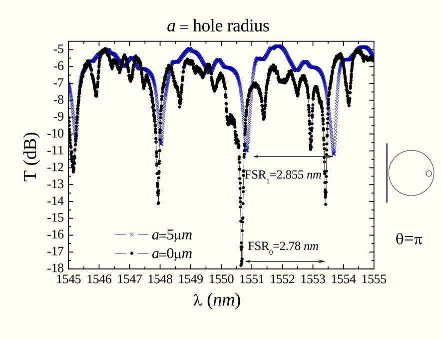

Fig. 8: **Transmission spectrum for a microcavity. Measurement from evanescent coupling with fiber taper.**

NSERC CRSNG
Fonds de recherche sur la nature et les technologies Québec